Nonlinear Dyn (2008) 51:245–258
DOI 10.1007/s11071-007-9207-4

ORIGINAL ARTICLE

Transient mode localization in coupled strongly nonlinear exactly solvable oscillators

V. N. Pilipchuk

Received: 20 September 2006 / Accepted: 5 January 2007 / Published online: 10 February 2007

Abstract Coupled strongly nonlinear oscillators, whose characteristic is close to linear for low amplitudes but becomes infinitely growing as the amplitude approaches certain limit, are considered in this paper. Such a model may serve for understanding the dynamics of elastic structures within the restricted space bounded by stiff constraints. In particular, this study focuses on the evolution of vibration modes as the energy is gradually pumped into or dissipates out of the system. For instance, based on the two degrees of freedom system, it is shown that the in-phase and out-of-phase motions may follow qualitatively different scenarios as the system' energy increases. So the in-phase mode appears to absorb the energy with equipartition between the masses. In contrast, the out-of-phase mode provides equal energy distribution only until certain critical energy level. Then, as a result of bifurcation of the 1:1 resonance path, one of the masses becomes a dominant energy receiver in such a way that it takes the energy not only from the main source but also from another mass.

Keywords Transient mode localization · Bifurcation of resonance manifold · Normal modes · Impact modes

V. N. Pilipchuk
Department of Theoretical and Applied Mechanics, National University, Dnepropetrovsk 49050, Ukraine
e-mail: valery.pilipchuk@yahoo.com

1 Introduction

The nonlinear mode localization has been known for a long time as both micro- and macro-level phenomenon, see for instance [1, 2] for earlier references and overview. In the area of nonlinear dynamics, mode localization recently became of a growing interest due to the idea of dynamic energy absorption [3–6]. In contrast to stochastic localization in disordered linear systems [7], nonlinear local modes may occur even in perfectly symmetric systems. In general terms, localization means that one or few particles become dynamically isolated from the rest of the system due to specific initial conditions and/or variation of physical parameters. Different analytical and numerical tools have been developed for both normal and local mode analyses [8]. However, comparatively less attention was paid to evolutionary/transient effects of nonlinear localization. On mathematical point of view, such kind of transient phenomena is developed in between the low- and high-energy asymptotics so that neither of them works well enough, although both steady-state limits can be matched in different phenomenological ways [9]. At this point, let us mention the results of numerical experiments on localized state formations, for instance [10]. As follows from Poicare recurrence theorem, in classic conservative systems, any inherent *one-way* energy localizations from distributed states are hardly sustainable. In order to observe such kind of phenomena, one must either insert nonconservative terms into the differential equations of motion or drastically increase

the number of degrees of freedom (DoFs) providing the recurrence time above any reasonable observation period.

In this work, the system is artificially made 'open' by generating the energy in-flow according to the negative damping law. Physically, this corresponds to conventional mechanisms of self-excitation before the system has reached the limit cycle. For instance, such kind of approaches can be relevant to modeling the friction-induced vibrations of elastic systems with clearances. It is shown that *transient localization admits interpretation as a passage through the bifurcation point of the 1:1 resonance manifold*. Explicit equations describing this phenomenon are obtained by using the unique class of strongly nonlinear oscillators with exact general solutions [11], see also [12, 13]. In particular, a strongly nonlinear coordinate transformation is introduced in terms of elementary functions. As a result, regular averaging procedures become applicable to a wide range of nonlinear motions including dynamic transitions from normal to local modes, and backward.

The paper is organized as follows. Section 2 describes the model of coupled oscillators and introduces the amplitude–phase coordinates for every oscillator. This brings the system to the form which is convenient for asymptotic analyses. In Section 3, the resonance manifold equation is obtained and discussed. Then, in Section 4, the differential equations of motion near the resonance manifold are obtained by adapting the conventional tool of averaging. The neighborhood of bifurcation of the 1:1 resonance path is analyzed in Section 5. Appendix A recalls some basic steps of the high-order averaging procedure adapted for strongly nonlinear systems in the standard Cauchy form. Necessary coefficients and other complicated expressions are listed in Appendix B.

2 System description

The model under investigation represents two linearly coupled strongly nonlinear oscillators. However, the original stage of transformations takes the compact form if applied to the corresponding multiple DoFs chain of oscillators

$$\ddot{x}_i + \frac{\tan x_i}{\cos^2 x_i} = \varepsilon(x_{i-1} - 2x_i + x_{i+1}) - \varepsilon\zeta\dot{x}_i \tag{1}$$

with the boundary conditions $x_0 \equiv x_{N+1} \equiv 0$, where $i = 1, \ldots, N$, and overdots indicate differentiation with respect to time t.

It is assumed that $0 < \varepsilon \ll 1$ and $|\zeta| \ll 1$; in other words, the damping is small compared to the strength of coupling.

Let us introduce new coordinates $\{\alpha_i, \varphi_i\}$ on the phase plane of every oscillator $\{x_i, \dot{x}_i\}$ by means of relationships

$$x_i = \arcsin(\alpha_i \sin\varphi_i)$$
$$\dot{x}_i = \frac{\alpha_i \Omega(\alpha_i) \cos\varphi_i}{\sqrt{1 - \alpha_i^2 \sin^2\varphi_i}} \tag{2}$$

where $|\alpha_i| < 1$ and

$$\Omega(\alpha_i) = \frac{1}{\sqrt{1 - \alpha_i^2}} \tag{3}$$

Transformation (2) is motivated by Nesterov's result [11] that the oscillator

$$\ddot{x}_i + \frac{\tan x_i}{\cos^2 x_i} = 0$$

has exact solution

$$x_i = \arcsin[\sin A_i \sin(t/\cos A_i)] \tag{4}$$

where A_i is a constant amplitude so that $\alpha_i = \sin A_i$.

If the amplitude A_i is close to zero, then the oscillator linearizes whereas solution (4) gives the corresponding sine-wave temporal shape. On the other hand, if the parameter A_i approaches the upper limit $\pi/2$, then the oscillation takes a triangular-wave shape while the period vanishes, as follows from expression (4). Such a high-energy limit corresponds to a free particle vibrating between the two stiff barriers on the interval $-\pi/2 < x_i < \pi/2$.

For an arbitrary energy level, the period and the total energy of the vibration are, respectively

$$T_i = 2\pi\sqrt{1 - \alpha_i^2} \tag{5}$$

and

$$E_i = \frac{1}{2}\frac{\alpha_i^2}{1 - \alpha_i^2} \tag{6}$$

Now, substituting (2) into (1) and imposing compatibility condition,

$$\frac{d\ \arcsin(\alpha_i\ \sin\ \varphi_i)}{dt} = \frac{\alpha_i \Omega(\alpha_i)\ \cos\ \varphi_i}{\sqrt{1-\alpha_i^2\ \sin^2\ \varphi_i}} \tag{7}$$

gives

$$\begin{aligned}\dot{\alpha}_i &= \varepsilon f(\alpha_{i-1}, \alpha_i, \alpha_{i+1}, \varphi_{i-1}, \varphi_i, \varphi_{i+1}) \cos\varphi_i \\ \dot{\varphi}_i &= \Omega(\alpha_i) - \frac{\varepsilon}{\alpha_i} f(\alpha_{i-1}, \alpha_i, \alpha_{i+1}, \varphi_{i-1}, \varphi_i, \varphi_{i+1}) \sin\varphi_i\end{aligned} \tag{8}$$

where

$$\begin{aligned}f(\alpha_{i-1}, \alpha_i, \alpha_{i+1}, \varphi_{i-1}, \varphi_i, \varphi_{i+1}) &= \frac{\Omega^{-3}(\alpha_i)}{\sqrt{1-\alpha_i^2\ \sin^2\ \varphi_i}} \\ &\times \Bigg[\arcsin(\alpha_{i-1}\ \sin\ \varphi_{i-1}) - 2\ \arcsin(\alpha_i \sin\varphi_i) \\ &+ \arcsin(\alpha_{i+1}\ \sin\ \varphi_{i+1}) - \frac{\zeta\alpha_i\Omega(\alpha_i)\ \cos\ \varphi_i}{\sqrt{1-\alpha_i^2\ \sin^2\ \varphi_i}} \Bigg]\end{aligned}$$

System (8) is still exactly equivalent to original system (1) regardless of the magnitudes of the parameter ε.

Further investigation focuses on 2 DOF system

$$\begin{aligned}\dot{\alpha}_i &= \varepsilon F_i(\alpha_1, \alpha_2, \varphi_1, \varphi_2) \\ \dot{\varphi}_i &= \Omega(\alpha_i) + \varepsilon G_i(\alpha_1, \alpha_2, \varphi_1, \varphi_2)\end{aligned} \tag{9}$$

where $i = 1, 2$, and expressions F_i and G_i are determined by (8).

In this case, let us introduce two new phase variables $\varphi(t)$ and $\theta(t)$ as follows:

$$\begin{aligned}\varphi_1 &= \varphi \\ \varphi_2 &= r\varphi + \theta\end{aligned} \tag{10}$$

where r is a constant ratio.

Assuming still no restrictions on the class of motions, relationships (10) bring the system to the form

$$\begin{aligned}\dot{\alpha}_i &= \varepsilon F_i(\alpha_1, \alpha_2, \varphi, r\varphi + \theta) \\ \dot{\varphi} &= \Omega(\alpha_1) + \varepsilon G_1(\alpha_1, \alpha_2, \varphi, r\varphi + \theta) \\ \dot{\theta} &= \Omega(\alpha_2) - r\Omega(\alpha_1) + \varepsilon[G_2(\alpha_1, \alpha_2, \varphi, r\varphi + \theta) \\ &\quad - rG_1(\alpha_1, \alpha_2, \varphi, r\varphi + \theta)]\end{aligned} \tag{11}$$

This is the standard Cauchy form of a strongly nonlinear vibrating system with two phase variables, φ and θ.

In order to formulate the major objective of further investigation, let us assume that there is some energy inflow into the system, for instance, due to the negative damping, $\zeta < 0$. It is clear that, at low energy level, the 2 DOF system possesses two linear modes dictated by the system's symmetry. On the other hand, as the total energy approaches infinity, the system becomes effectively decoupled. As a result, four different impact modes become possible, such as in-phase, out-of-phase, and a couple of localized modes with one of the two oscillators remaining in rest. The objective is to clarify the scenario of transition from the normal to impact mode dynamics. On this point of view, the geometry of resonance curves on the configuration plane appears to play an important role as follows from the analyses below.

3 Structure of the resonance manifold

By differentiating both sides of expressions (10) with respect to time, one obtains

$$\frac{\dot{\varphi}_2}{\dot{\varphi}_1} = r + \frac{\dot{\theta}}{\dot{\varphi}} \tag{12}$$

Therefore, the system is close to the resonance of a frequency ratio r if and only if the variable θ is slow compared to φ so that

$$\frac{\dot{\theta}}{\dot{\varphi}} \ll r \tag{13}$$

This condition implies that, during the motion, the right-hand side of the last equation in (11) remains sufficiently small compared to that of the second equation. Perfectly, the exact resonance condition is satisfied on the resonance manifold $\dot{\theta} = 0$ or

$$\begin{aligned}&\Omega(\alpha_2) - r\Omega(\alpha_1) + \varepsilon[G_2(\alpha_1, \alpha_2, \varphi, r\varphi) \\ &\quad - rG_1(\alpha_1, \alpha_2, \varphi, r\varphi)] = 0 \\ &\theta = 0\end{aligned} \tag{14}$$

where the initial condition $\theta(0) = 0$ is imposed.

Despite simplicity of the expression $\Omega(\alpha_i)$, the entire Equation (14) is still complicated for visualization and further analyses. However, since resonances are determined by information about entire vibration cycles, then the dimension of the manifold can be reduced by averaging the resonance condition with respect to the explicit phase φ

$$\Omega(\alpha_2) - r\Omega(\alpha_1) + \varepsilon < G_2(\alpha_1, \alpha_2, \varphi, r\varphi) - rG_1(\alpha_1, \alpha_2, \varphi, r\varphi) >= 0 \quad (15)$$

Here and below, $\langle\bullet\rangle$ is a mean value on the interval $0 \le \varphi \le 2\pi$:

$$\langle\bullet\rangle \equiv \frac{1}{2\pi}\int_0^{2\pi}(\bullet)\,d\varphi$$

Equation (15) describes a family of resonance curves with the frequency ratio r on the configuration plane

$$K = \{(\alpha_1, \alpha_2) : |\alpha_1| < 1,\ |\alpha_2| < 1\} \quad (16)$$

Note that it is *a priori* difficult to determine whether or not some resonance curve will attract the system, and therefore, provide Equation (15) with a real physical meaning. On that point of view, it is important to clarify both the geometry of curves (15) and the system dynamics near the curves.

Geometrical representation of Equation (15) is given in Figs. 1 and 2 for perfectly decoupled and weakly coupled oscillators, respectively. Central areas of both diagrams are occupied by 1:1 resonance lines, $r = 1$. In both figures, the vertical and horizontal straight lines $\alpha_1 = 0$ and $\alpha_2 = 0$, respectively, correspond to the localized modes of the decoupled system, $\varepsilon = 0$. The diagonals $\alpha_2 = \alpha_1$ and $\alpha_2 = -\alpha_1$ represent the in-phase and out-of-phase modes, respectively. Both these modes belong, of course, to the 1:1 resonance manifold. In the case of nonzero coupling, there are also two 1:1 curvilinear resonance lines bifurcating from the out-of-phase mode, and then, asymptotically approaching the localized modes as shown in Fig. 2. Such a bifurcation, which is important for understanding the transient localization, cannot be captured by the limit of decoupled oscillators, as follows from Fig. 1.

Let us consider the limit case analytically. Setting $\varepsilon = 0$ in Equation (15) and taking into account expression (3) gives

$$\alpha_1^2 - r^2\alpha_2^2 = 1 - r^2 \quad (17)$$

This equation describes a family of hyperbolas in K. In particular case $r = 1$, Equation (17) describes only the in-phase and out-of-phase modes, $\alpha_2 = \pm\alpha_1$. Due to the symmetry of the coupled system, the diagonals satisfy also the entire Equation (15) with $\varepsilon \neq 0$.

4 Dynamics near the resonance manifold

4.1 Local coordinates

Let us introduce local coordinates $\{\rho, s\}$ on the resonance curves of the decoupled system as

$$\alpha_1(\rho, s) = x_1(s) + \rho n_1(s)$$
$$\alpha_2(\rho, s) = x_2(s) + \rho n_2(s) \quad (18)$$

where $\{x_1(s), x_2(s)\}$ is an arbitrary point on curve (17) defined by the parameter s, and the normal vector $\{n_1(s), n_2(s)\}$ is normalized to unity in terms of the euclidean distance in K.

Equations (11) then take the form

$$\begin{aligned}
\dot\rho &= \varepsilon R(\rho, s, \varphi, \theta)\\
\dot s &= \varepsilon S(\rho, s, \varphi, \theta)\\
\dot\theta &= \Omega[\alpha_2(\rho, s)] - r\Omega[\alpha_1(\rho, s)] + \varepsilon\Theta(\rho, s, \varphi, \theta)\\
\dot\varphi &= \Omega[\alpha_1(\rho, s)] + \varepsilon G(\rho, s, \varphi, \theta)
\end{aligned} \quad (19)$$

where

$$\begin{aligned}
R(\rho, s, \varphi, \theta) &= n_1(s)F_1 + n_2(s)F_2\\
S(\rho, s, \varphi, \theta) &= \frac{x_1'(s)F_1 + x_2'(s)F_2}{[x_1'(s)]^2 + [x_2'(s)]^2 + \rho[n_1'(s)x_1'(s) + n_2'(s)x_2'(s)]}\\
\Theta(\rho, s, \varphi, \theta) &= G_2 - rG_1\\
G(\rho, s, \varphi, \theta) &= G_1\\
F_i &= F_i(\alpha_1(\rho, s), \alpha_2(\rho, s), \varphi, r\varphi + \theta)\\
G_i &= G_i(\alpha_1(\rho, s), \alpha_2(\rho, s), \varphi, r\varphi + \theta)\\
' &\equiv d/ds
\end{aligned}$$

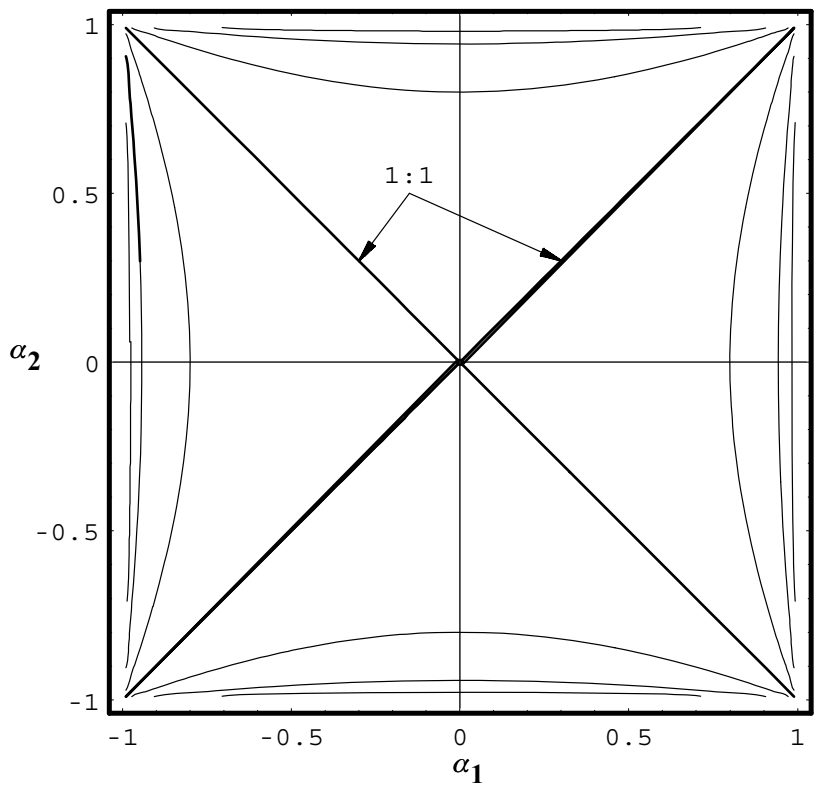

Fig. 1 Resonance curves of the decoupled system, $\varepsilon = 0$, for frequency ratios $r = 1, 1/3, 3, 1/5, 5, 3/5,$ and $5/3$

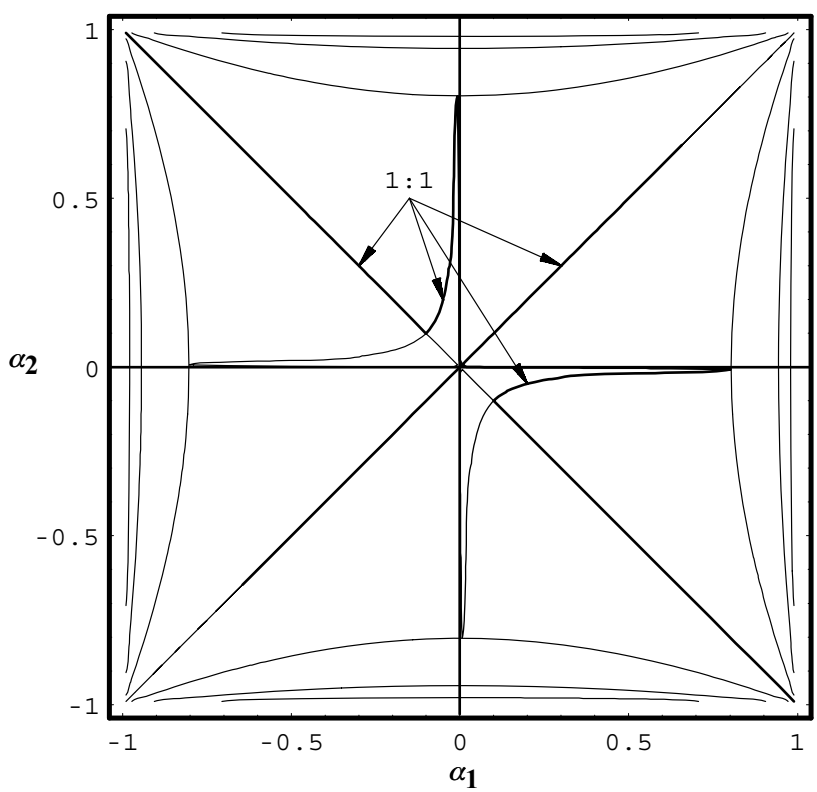

Fig. 2 Resonance curves of the weakly coupled oscillators, $\varepsilon = 0.01$, for frequency ratios $r = 1, 1/3, 3, 1/5, 5, 3/5,$ and $5/3$

Equations (19) finalize the transformation of variables

$$\{\alpha_1, \alpha_2, \varphi_1, \varphi_2\} \longrightarrow \{\rho, s, \varphi, \theta\}$$

These equations are still exact but appear to complicate the original form of equations. Nevertheless, the major advantage of the new system is due to the explicit presence of the distance ρ to lines (17). This fact will essentially be employed below.

4.2 Asymptotic analysis and discussion

Let us bring the system to the standard form with a single fast phase. At this point, first physical assumption is introduced. Namely, it is assumed that $\rho \sim \mu = \sqrt{\varepsilon}$; in other words, the whole system remains near the resonance lines of the decoupled system. Then, by rescaling the distance as $\rho = \mu l$, one obtains

$$\begin{aligned}
\dot{l} &= \mu R(\mu l, s, \varphi, \theta) \\
\dot{s} &= \mu^2 S(\mu l, s, \varphi, \theta) \\
\dot{\theta} &= \mu Q(l, s) + \mu^2 \Theta(\mu l, s, \varphi, \theta) \\
\dot{\varphi} &= \Omega(\mu l, s) + \mu^2 G(\mu l, s, \varphi, \theta)
\end{aligned} \tag{20}$$

where $\mu Q(l, s) = \Omega[x_2(s) + \mu l n_2(s)] - r\Omega[x_1(s) + \mu l n_1(s)] = O(\mu)$, and $\Omega(\mu l, s) \equiv \Omega[x_1(s) + \mu l n_1(s)]$.

The system now has a single fast phase φ and should be qualified as an 'essentially nonlinear' system due to the *essential* dependance of its basic frequency Ω on the system's position.

Second-order averaging with respect to the fast phase, which is described in Appendix A, gives the coordinate transformation and the corresponding differential equations of motion in, respectively, the form

$$\begin{aligned}
l &= q + \frac{\mu}{\Omega(\mu q, p)} \int_0^{\varphi} [R(\mu q, p, \varphi, \theta) \\
&\quad - \langle R(\mu q, p, \varphi, \theta) \rangle] \, d\varphi \\
s &= p + \frac{\mu^2}{\Omega(\mu q, p)} \int_0^{\varphi} [S(\mu q, p, \varphi, \theta) \\
&\quad - \langle S(\mu q, p, \varphi, \theta) \rangle] \, d\varphi
\end{aligned} \tag{21}$$

and

$$\begin{aligned}
\dot{q} &= \mu \langle R(\mu q, p, \varphi, \theta) \rangle \\
\dot{p} &= \mu^2 \langle S(\mu q, p, \varphi, \theta) \rangle \\
\dot{\theta} &= \mu Q(q, p) + \mu^2 \langle \Theta(\mu q, p, \varphi, \theta) \rangle \\
\dot{\varphi} &= \Omega(\mu q, p) + \mu^2 \langle G(\mu q, p, \varphi, \theta) \rangle
\end{aligned} \tag{22}$$

Taking into account the Fourier expansions for R, S, Θ, and G with respect to the phase angle φ and calculating the integrals in (22) gives

$$\begin{aligned}
\dot{q} &= \mu [R_0(\mu q, p) + R_1(\mu q, p) \sin\theta \\
&\quad + R_3(\mu q, p) \sin 3\theta + \cdots] \\
\dot{p} &= \mu^2 [S_0(\mu q, p) + S_1(\mu q, p) \sin\theta \\
&\quad + S_3(\mu q, p) \sin 3\theta + \cdots] \\
\dot{\theta} &= \mu Q(q, p) + \mu^2 [\Theta_0(\mu q, p) + \Theta_1(\mu q, p) \cos\theta \\
&\quad + \Theta_3(\mu q, p) \cos 3\theta + \cdots] \\
\dot{\varphi} &= \Omega(\mu q, p) + \mu^2 [G_0(\mu q, p) + G_1(\mu q, p) \cos\theta \\
&\quad + G_3(\mu q, p) \cos 3\theta + \cdots]
\end{aligned} \tag{23}$$

where the coefficients are listed in Appendix B.

This is a final result of the averaging procedure that separated fast and slow components of the dynamics. Further calculations require parametrization of curves (17). In this work, only the case of 1:1 resonance is considered, when $r = 1$ and Equation (17), therefore, gives diagonals $\alpha_2 = \alpha_1$ and $\alpha_2 = -\alpha_1$ in K corresponding to in-phase and out-of-phase normal modes, respectively. For example, the out-of-phase mode admits the parametrization $x_1(s) = -s$ and $x_2(s) = s$ with the related normal vector $\{n_1, n_2\} = (\sqrt{2}/2)\{1, 1\}$ so that the coordinate transformation (18) takes the form

$$\begin{aligned}
\alpha_1 &= -s + \rho\sqrt{2}/2 = -s + \mu l\sqrt{2}/2 \\
\alpha_2 &= s + \rho\sqrt{2}/2 = s + \mu l\sqrt{2}/2
\end{aligned} \tag{24}$$

Since the coordinates s and $\rho = \mu l$ are described by Equations (21) then (24) gives

$$\begin{aligned}
\alpha_1 &= -p + \mu q\sqrt{2}/2 + O(\mu^2) \\
\alpha_2 &= p + \mu q\sqrt{2}/2 + O(\mu^2)
\end{aligned} \tag{25}$$

Let us first discuss the results of numerical integration of system (23). In Fig. 3, the dashed lines represent 1:1 resonances as those shown in Fig. 2 on the amplitude plane K. Therefore, the horizontal and vertical dashed straight lines are pieces of the in-phase and out-of-phase modes, respectively. Two another dashed curves intersect the out-of-phase mode. Along these curves, the system can eventually reach the localized modes with no violation of the 1:1 resonance condition. So, every such intersection qualifies as a bifurcation point of the 1:1 resonance manifold. The purpose of numerical tests was to clarify the global system behavior near the 1:1 resonance lines including the above bifurcation points.

First, the numerical simulations suggest instability of the out-of-phase mode above the bifurcation point. In particular, Fig. 3 shows that the system leaves the neighborhood of the out-of-phase mode on considerable distance from the initial position regardless of the initial distance to the mode. Nevertheless, globally, the out-of-phase mode remains attractive to the system, as Fig. 4 clearly shows.

Now, let us assume that the energy is pumped into the system according to the negative damping law (see the introductory remarks for a physical interpretation of this assumption). Let initially the system be close to the out-of-phase mode below the bifurcation point. While the energy is slowly pumped into the system, its path remains close to the out-of phase mode for some period of time. At some energy level, however, the out-of-phase mode fails to attract the system and further energy partition qualitatively changes, as shown in Figs. 5 and 6. The system prefers to take another branch of the 1:1 resonance manifold so that the energy obtained by the system is not equally distributed any more between the two particles. For instance, Fig. 7 shows that particle 1 becomes the dominant energy receiver taking back even some energy accumulated by another particle before the symmetry brake has occurred.

The system's behavior during the localization process appears to be reversible under the positive damping condition (see Figs. 8 and 9). In particular, despite the positive damping, the energy of particle 1 *is growing* until it becomes equal to that of particle 2. Then, the energy becomes equally dissipating out of both particles, as shown in Fig. 9.

5 Dynamics near the bifurcation point: Onset of localization

In order to understand the above numerical results, let us consider the neighborhood of bifurcation point by assuming that the distance from the origin to the bifurcation point is of the order $\mu = \sqrt{\varepsilon}$. This is justified in the case of weak coupling between the oscillators. Indeed, if no coupling at all, $\varepsilon = 0$, the bifurcation points are absorbed by the equilibrium position (see Figs. 1 and 2). Based on the above assumption, let us rescale the coordinate along the out-of-phase mode

$$p = \sqrt{\varepsilon} P \tag{26}$$

Now, linearizing Equations (23) with respect to q and θ and keeping the leading-order terms with respect to ε gives

$$\frac{d}{dt}\begin{bmatrix} q \\ \theta \end{bmatrix} = \varepsilon \begin{bmatrix} -\zeta/2 & \sqrt{2}P/2 \\ \sqrt{2}(P - P^{-1}) & 0 \end{bmatrix} \begin{bmatrix} q \\ \theta \end{bmatrix} \tag{27}$$

and

$$\dot{P} = -\frac{1}{2}\zeta \varepsilon P \tag{28}$$

The equation for phase φ is not considered; however, the equation for θ is included in order to track the resonance condition $\theta = 0$. As seen from Equation (27), the condition $\theta \equiv 0$ may be satisfied while the system remains on the out-of-phase mode $q = 0$.

Equation (28) describes the amplitude of the out-of-phase mode as a slow varying exponential function

$$P = P_0 \exp\left(-\frac{1}{2}\zeta \varepsilon t\right) \tag{29}$$

where $P_0 = P(0)$.

By considering P as a quasi-constant parameter, one can determine the type of equilibrium point of system (27) as the system slowly drifts along the resonance manifold $\theta = 0$, or $(P - P^{-1})q = 0$. In particular, it is seen that the resonance manifold bifurcates at $P = \pm 1$ in such a way that a nonzero in-phase component q may occur with no violation of the 1:1 resonance condition. This indicates an onset of the localization phenomenon, which can be described as a growing in-phase mode

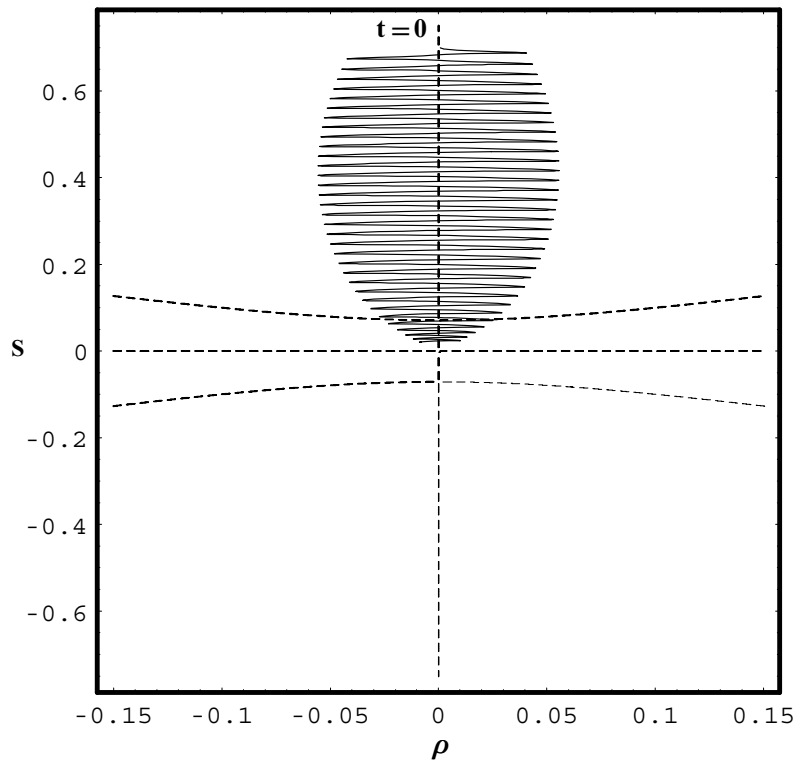

Fig. 3 Global dissipative dynamics of weakly coupled oscillators near the out-of-phase mode on the 'amplitude plane' under the following parameters and initial conditions: $\varepsilon = 0.005$, $\zeta = 0.1$, $\rho(0) = 0.001$, $s(0) = 0.7$, $\theta(0) = 0.0$, $\varphi(0) = 0.0$, and $T_{\max} = 15000.0$

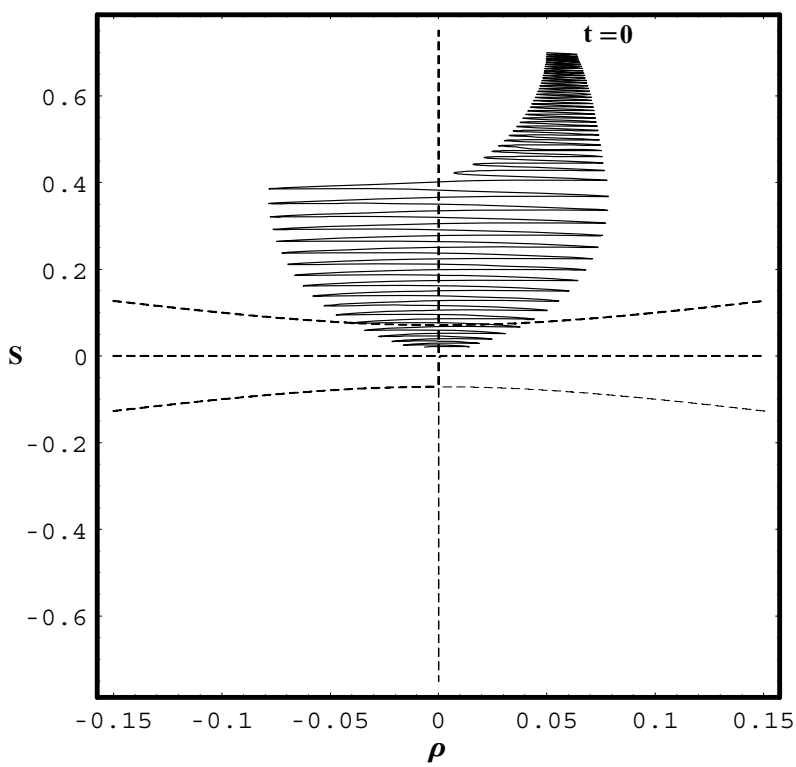

Fig. 4 Global dissipative dynamics of the weakly coupled oscillators near the out-of-phase mode on the 'amplitude plane' under the following parameters and initial conditions: $\varepsilon = 0.005$, $\zeta = 0.1$, $\rho(0) = 0.05$, $s(0) = 0.7$, $\theta(0) = 0.0$, $\varphi(0) = 0.0$, and $T_{\max} = 15000.0$

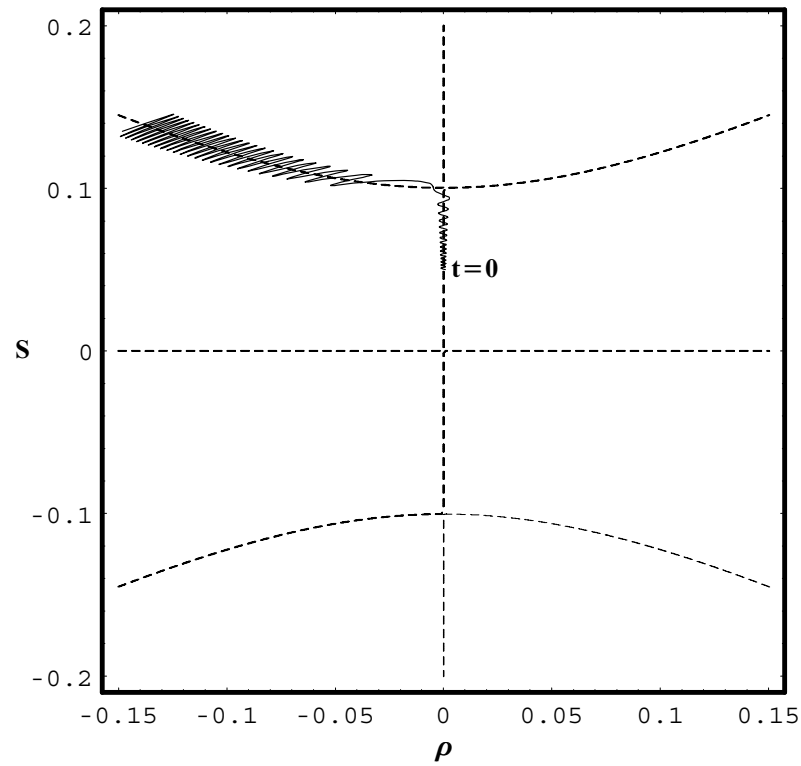

Fig. 5 Transient mode localization under the energy inflow due to negative damping. The parameters are as follows: $\varepsilon = 0.01$, $\zeta = -0.01$, $\rho(0) = 0.001$, $s(0) = 0.05$, $\theta(0) = 0.0$, $\varphi(0) = 0.0$, and $T_{\max} = 25000.0$

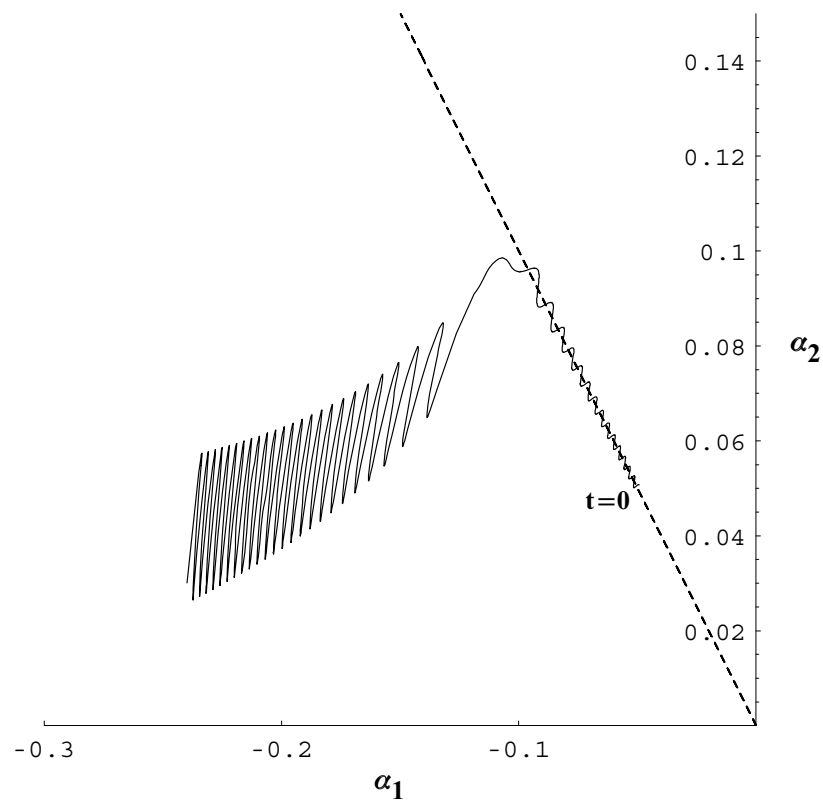

Fig. 6 Magnified portion of the previous figure transformed to the original 'amplitude plane' $\alpha_1\alpha_2$

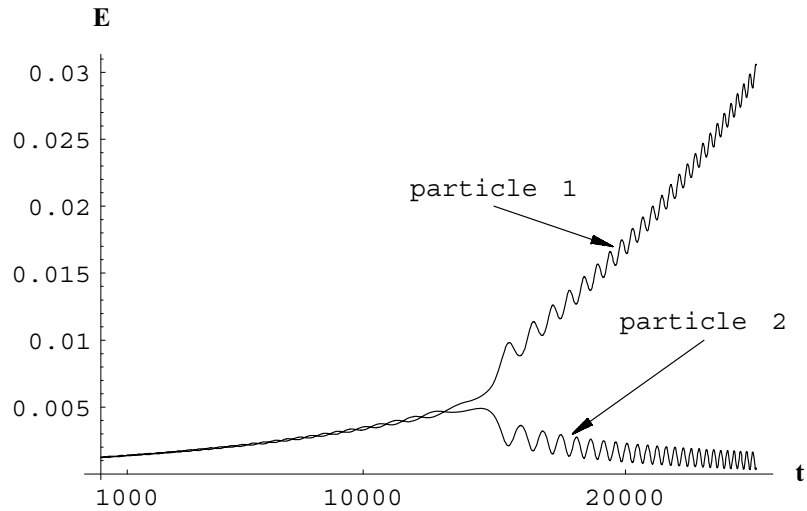

Fig. 7 Representation of the transient localization on the energy versus time plane

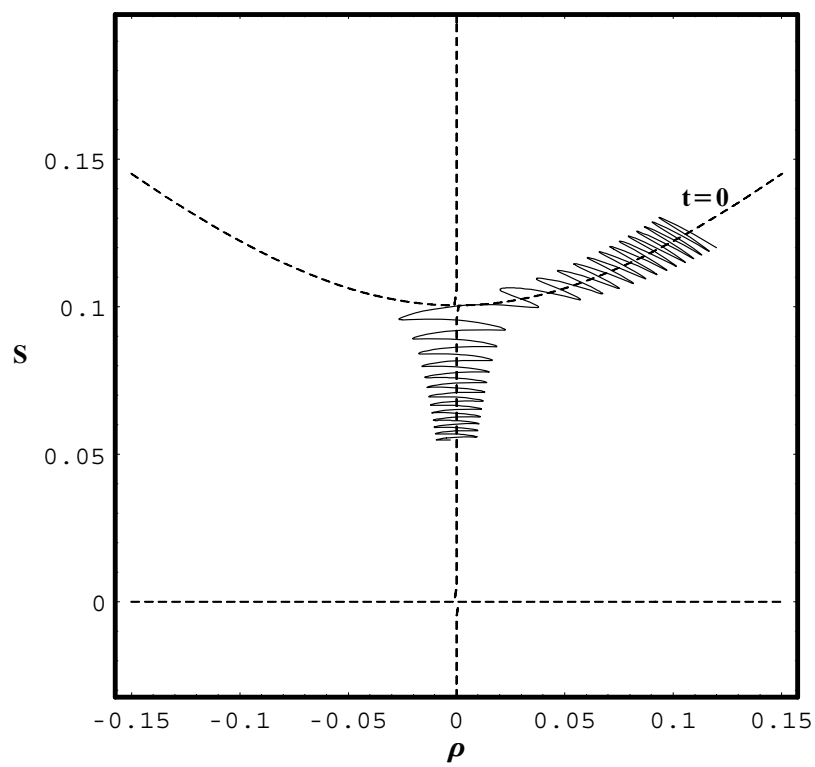

Fig. 8 The transient dynamics from local to out-of-phase normal mode due to energy loss. The parameters are as follows: $\varepsilon = 0.01$, $\zeta = 0.01$, $\rho(0) = 0.12$, $s(0) = 0.12$, $\theta(0) = 0.0$, $\varphi(0) = 0.0$, and $T_{\max} = 20000.0$

near the bifurcation point. Eliminating the phase θ from system (27) gives

$$\ddot{q} + \zeta\varepsilon\dot{q} + \varepsilon^2\left(1 + \frac{1}{4}\zeta^2 - P^2\right)q = 0 \tag{30}$$

As the coordinate P is 'frozen,' the corresponding characteristic equation has a couple of roots

$$\lambda_{1,2} = \varepsilon\left(-\frac{1}{2}\zeta \pm i\sqrt{1 - P^2}\right) \tag{31}$$

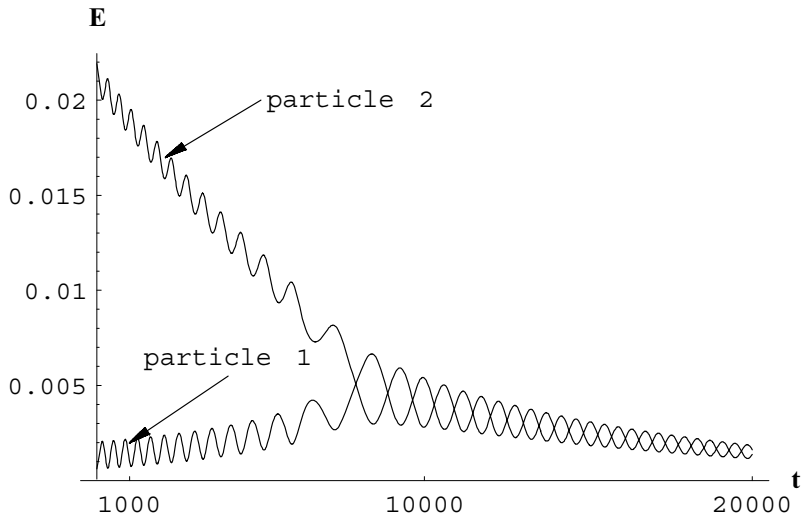

Fig. 9 Transition from the localized to cooperative dynamics on the energy versus time plane

These roots determine the phase portrait of in-phase dynamics near the out-of-phase mode.

Let us consider the case of negative damping $\zeta < 0$ under the assumption $0 < P_0 < 1$. In this case, as follows from (31), the out-of-phase mode is always unstable. However, as P grows according to (29), the type of instability is changing as follows:

(a) $0 < P < 1$ (*unstable focus*): The in-phase component oscillates with a slowly increasing amplitude.
(b) $1 < P < 1 + \zeta^2/4$ (*unstable node*): There is no more oscillations about the out-of-phase mode; however, the in-phase modal amplitude still grows at a slow rate $\varepsilon|\zeta|$.
(c) $1 + \zeta^2/4 < P$ (*saddle point*): The in-phase amplitude growth drastically accelerates because the stiffness of oscillator (30) becomes negative. The system drifts now along another branch of the resonance manifold leading to localization.

In the case of positive damping $\zeta > 0$, let us assume that the system is initially above the bifurcation point $P_0 > 1 + \zeta^2/4$. As P slowly decreases according to (29), the type of equilibrium point is changing as follows:

(a) $1 + \zeta^2/4 < P$ (*saddle point*),
(b) $1 < P < 1 + \zeta^2/4$ (*stable node*),
(c) $0 < P < 1$ (*stable focus*).

Numerical tests on the corresponding nonlinear system confirm all qualitative features of the local behavior near the out-of-phase mode as described by the linearized model (30). However, the linearized model does not capture some properties of the global dynamics near the locally unstable region. In particular, the in-phase amplitude increase is limited by a global cycle as follows from Figs. 3 and 4.

So, the original system reveals a hierarchy of three different temporal scales of the dynamics. The fastest scale associated with the temporal rate of fast phase was excluded by the averaging. Then, the dynamic process described by system (27) is developed in a slow scale determined by the parameter of coupling ε. Finally, as follows from Equation (28), the coefficients of system (27) are varying at the slowest rate estimated by the damping coefficient $\zeta\varepsilon$.

6 Concluding remarks

In this work, regular perturbation approaches to strongly nonlinear transient dynamics have been developed based on exactly solvable oscillators. The developed tool was applied to tracking the mode localization and delocalization phenomena in the 2 DOF system as the energy is slowly pumped into or out of the system, respectively. In particular, it was shown that the onset of localization is associated with the bifurcation of 1:1 resonance manifold on the out-of-phase mode such that the phase diagram of the in-phase component passes

paths through unstable node to saddle point. Once the amplitude of in-phase mode has reached the order of out-of-phase mode, the energy becomes localized on one of the two masses.

Although this study is based on the oscillators with specific restoring force characteristics, the phenomenon itself seems to have a general meaning. As a further extension of this work, a coupled set of oscillators with arbitrary hardening characteristics could be considered. Also, it would be important to increase the number of DoFs by one, at least in order to find a three-dimensional version of the transient localization.

Appendix A

Let us specify the system as follows

$$\begin{aligned}
\dot{l} &= \mu R(\mu l, s, \varphi, \theta) \\
\dot{s} &= \mu^2 S(\mu l, s, \varphi, \theta) \\
\dot{\theta} &= \mu Q(l, s) + \mu^2 \Theta(\mu l, s, \varphi, \theta) \\
\dot{\varphi} &= \Omega(\mu l, s) + \mu^2 G(\mu l, s, \varphi, \theta)
\end{aligned} \tag{A.1}$$

where μ is a small parameter.

Such kind of equations may occur when considering 'essentially nonlinear' systems with state-dependent frequencies under different resonance conditions.

Below, the averaging tool described in [14] is adapted to the specific class of systems (A.1).

First approximation is obtained by keeping first-order terms on the right-hand side of system (A.1) and applying the averaging procedure with respect to the fast phase φ. This gives

$$\begin{aligned}
\dot{l} &= \mu \langle R(0, s_0, \varphi, \theta) \rangle \\
\dot{\theta} &= \mu Q(l, s_0)
\end{aligned} \tag{A.2}$$

where s_0 is constant in first order with respect to μ.

System (A.2) is easily integrated and the result gives an error of order μ on time intervals of order $1/\mu$. In many cases, however, first approximation may give incomplete characterization of the system.

In order to illustrate the next step, let us consider only first equation of system (A.1). This is sufficient for illustration of the procedure which is sequentially applied in the same way to other equations. Let us represent the first equation of (A.1) in the form

$$\begin{aligned}
\dot{l} = \mu \langle R(0, s_0, \varphi, \theta) \rangle + \mu [R(0, s, \varphi, \theta) \\
- \langle R(0, s_0, \varphi, \theta) \rangle] + \mu^2 l R'_\rho(0, s_0, \varphi, \theta) + O(\mu^3)
\end{aligned} \tag{A.3}$$

Following the idea of averaging, one must eliminate the second term on the right-hand side by means of the coordinate transformation

$$l = q + \mu f(q, s, \varphi, \theta) \tag{A.4}$$

Substituting (A.4) into (A.3) and taking into account (A.1) gives

$$\begin{aligned}
&\dot{q} + \mu \left(\frac{\partial f}{\partial q} \dot{q} + \frac{\partial f}{\partial s} \dot{s} + \frac{\partial f}{\partial \varphi} \dot{\varphi} + \frac{\partial f}{\partial \theta} \dot{\theta} \right) \\
&\quad = \mu \langle R(0, s, \varphi, \theta) \rangle + \mu [R(0, s, \varphi, \theta) \\
&\qquad - \langle R(0, s, \varphi, \theta) \rangle] + \mu^2 q R'_\rho(0, s, \varphi, \theta) + O(\mu^3)
\end{aligned} \tag{A.5}$$

Now, the function $f(q, s, \varphi, \theta)$ is determined from the condition

$$\Omega(0, s) \frac{\partial f}{\partial \varphi} = R(0, s, \varphi, \theta) - \langle R(0, s, \varphi, \theta) \rangle \tag{A.6}$$

which eliminates the fast phase φ from the equation in first order of μ.

Further, $f(q, s, \varphi, \theta)$ must be independent of q because the terms of order μ on the right-hand side of Equation (A.6) do not depend on q. As a result, Equation (A.5) takes the form

$$\begin{aligned}
\dot{q} = \mu \langle R(0, s, \varphi, \theta) \rangle + \mu^2 q R'_\rho(0, s, \varphi, \theta) \\
- \mu^2 \left(\frac{\partial f}{\partial \varphi} q \Omega'_\rho(0, s) + \frac{\partial f}{\partial \theta} Q(q, s) \right) + O(\mu^3)
\end{aligned} \tag{A.7}$$

Since the fast phase φ has been eliminated from the terms of order μ, then the averaging procedure applies to the terms of order μ^2 analogously to the first stage of the method. So, taking into account the obvious relationship $\langle \partial f / \partial \varphi \rangle = \langle \partial f / \partial \theta \rangle = 0$ gives

$$\dot{q} = \mu \langle R(0, s, \varphi, \theta) \rangle + \mu^2 \langle q R'_\rho(0, s, \varphi, \theta) \rangle + O(\mu^3)$$

Within the same order of magnitudes, the above equation is equivalent to

$$\dot{q} = \mu\langle R(\mu q, s, \varphi, \theta)\rangle + O(\mu^3) \tag{A.8}$$

The second approximation, therefore, is a direct averaging of the original Equation (A.1); however, the original coordinate l is expressed by transformation (A.4), which is determined by (A.6) in the form

$$l = q + \frac{\mu}{\Omega(\mu q, s)} \int_0^{\varphi} (R(\mu q, s, \varphi, \theta) - \langle R(\mu q, s, \varphi, \theta)\rangle)\, d\varphi + O(\mu^2) \tag{A.9}$$

In this expression, the variable μq is back instead of zero. Although the expression still approximates the coordinate transformation in first order of μ, its form becomes compliant with Equation (A.8). Moreover, such a modification often improves results of calculation.

Appendix B

In order to analytically calculate the integrals of averaging, the trigonometric expansions are used as follows:

$$\frac{1}{\sqrt{1 - z^2 \sin^2 \varphi}} = \sum_{k=0}^{1} A_{2k}(z) \cos 2k\varphi, \quad |z| < 1 \tag{B.1}$$

$$A_0 = 2\frac{K}{\pi}$$

$$A_2 = 4\frac{2E + (z^2 - 2)K}{\pi z^2}$$

$$\arcsin(z \sin \varphi) = \sum_{k=1}^{2} B_{2k-1}(z) \sin(2k-1)\varphi \tag{B.2}$$

$$B_1 = z + \frac{1}{8}z^3 + \frac{3}{64}z^5 + \frac{25}{1024}z^7 + \frac{245}{16384}z^9 + O(z^{11})$$

$$B_3 = -\frac{1}{24}z^3 - \frac{3}{128}z^5 - \frac{15}{1024}z^7 - \frac{245}{24576}z^9 + O(z^{11})$$

$$\frac{\cos \varphi}{1 - z^2 \sin^2 \varphi} = \sum_{k=1}^{5} Q_{2k-1}(z) \sin(2k-1)\varphi \tag{B.3}$$

$$Q_1 = \frac{2}{z^2\sqrt{(1-z^2)}}\left[-1 + z^2 + \sqrt{(1-z^2)}\right]$$

$$Q_3 = \frac{2}{z^4\sqrt{(1-z^2)}}[4 - 5z^2 + z^4 + (3z^2 - 4)\sqrt{(1-z^2)}]$$

where $K = K(z^2)$ is the complete elliptic integral of the first kind, and $E = E(z^2)$ is the complete elliptic integral.

Note that the coefficients of expansion (B.1) are exact, and therefore, the essentially nonlinear specific of the system is preserved.

Coefficients of the averaged equations are listed as follows:

$$R_0 = -\frac{\zeta}{2}\left[\frac{n_1 Q_1(\alpha_1)\alpha_1}{\Omega(\alpha_1)^2} + \frac{n_2 Q_1(\alpha_2)\alpha_2}{\Omega(\alpha_2)^2}\right]$$

$$R_1 = \frac{1}{4}\left[\frac{n_1[2A_0(\alpha_1) + A_2(\alpha_1)]B_1(\alpha_2)}{\Omega(\alpha_1)^2} - \frac{n_2[2A_0(\alpha_2) + A_2(\alpha_2)]B_1(\alpha_1)}{\Omega(\alpha_2)^2}\right]$$

$$R_3 = \frac{1}{4}\left[\frac{n_1 A_2(\alpha_1)B_3(\alpha_2)}{\Omega(\alpha_1)^2} - \frac{n_2 A_2(\alpha_2)B_3(\alpha_1)}{\Omega(\alpha_2)^2}\right]$$

$$S_0 = -\frac{\zeta}{2}\left[\frac{\partial x_1}{\partial s}\frac{Q_1(\alpha_1)\alpha_1}{\Omega(\alpha_1)^2} + \frac{\partial x_2}{\partial s}\frac{Q_1(\alpha_2)\alpha_2}{\Omega(\alpha_2)^2}\right] \times \left(\frac{\partial x_1}{\partial s}\frac{\partial \alpha_1}{\partial s} + \frac{\partial x_2}{\partial s}\frac{\partial \alpha_2}{\partial s}\right)^{-1}$$

$$S_1 = \frac{1}{4}\left[\frac{\partial x_1}{\partial s}\frac{[2A_0(\alpha_1) + A_2(\alpha_1)]B_1(\alpha_2)}{\Omega(\alpha_1)^2} - \frac{\partial x_2}{\partial s}\frac{[2A_0(\alpha_2) + A_2(\alpha_2)]B_1(\alpha_1)}{\Omega(\alpha_2)^2}\right] \times \left(\frac{\partial x_1}{\partial s}\frac{\partial \alpha_1}{\partial s} + \frac{\partial x_2}{\partial s}\frac{\partial \alpha_2}{\partial s}\right)^{-1}$$

$$S_3 = \frac{1}{4}\left[\frac{\partial x_1}{\partial s}\frac{A_2(\alpha_1)B_3(\alpha_2)}{\Omega(\alpha_1)^2} - \frac{\partial x_2}{\partial s}\frac{A_2(\alpha_2)]B_3(\alpha_1)}{\Omega(\alpha_2)^2}\right] \times \left(\frac{\partial x_1}{\partial s}\frac{\partial \alpha_1}{\partial s} + \frac{\partial x_2}{\partial s}\frac{\partial \alpha_2}{\partial s}\right)^{-1}$$

$$G_0 = \frac{2A_0(\alpha_1)B_1(\alpha_1) + A_2(\alpha_1)[B_3(\alpha_1) - B_1(\alpha_1)]}{2\Omega(\alpha_1)^3\alpha_1}$$

$$G_1 = \frac{[-2A_0(\alpha_1) + A_2(\alpha_1)]B_1(\alpha_2)}{4\Omega(\alpha_1)^3\alpha_1}$$

$$G_3 = -\frac{A_2(\alpha_1)B_3(\alpha_2)}{4\Omega(\alpha_1)^3\alpha_1}$$

$$\Theta_0 = \frac{-2A_0(\alpha_1)B_1(\alpha_1) + A_2(\alpha_1)[B_3(\alpha_1) - B_1(\alpha_1)]}{2\Omega(\alpha_1)^3\alpha_1} + \frac{2A_0(\alpha_2)B_1(\alpha_2) + A_2(\alpha_2)[B_3(\alpha_2) - B_1(\alpha_2)]}{2\Omega(\alpha_2)^3\alpha_2}$$

$$\Theta_1 = \frac{[2A_0(\alpha_1) - A_2(\alpha_1)]B_1(\alpha_2)}{4\Omega(\alpha_1)^3\alpha_1} + \frac{[-2A_0(\alpha_2) + A_2(\alpha_2)]B_1(\alpha_1)}{4\Omega(\alpha_2)^3\alpha_2}$$

$$\Theta_3 = \frac{A_2(\alpha_1)B_3(\alpha_2)}{4\Omega(\alpha_1)^3\alpha_1} - \frac{A_2(\alpha_2)B_3(\alpha_1)}{4\Omega(\alpha_2)^3\alpha_2}$$

References

1. Jaffe, C., Brumer, P.: Local and normal modes: a classical perspective. J. Chem. Phys. **73**(11), 5646–5658 (1980)
2. Manevich, L.I., Pilipchuk, V.N.: Localization of oscillations in linear and nonlinear chains. Adv. Mech. **13**(3/4), 107–134 (1990)
3. Ormondroyd, J., Den Hartog, J.: The theory of the dynamic vibration absorber. Trans. Am. Soc. Mech. Eng. **50**, A9–A22 (1928)
4. Den Hartog, J.: Mechanical Vibration. McGraw-Hill, New York (1947)
5. Roberson, R.: Synthesis of a nonlinear dynamic vibration absorber. J. Franklin Inst. **254**, 205–220 (1952)
6. Lee, Y., Kerschen, G., Vakakis, A., Panagopoulos, P., Bergman, L., McFarland, D.: Complicated dynamics of a linear oscillator with a light, essentially nonlinear attachment. Physica D **204**, 41–69 (2005)
7. Pierre, C., Castanier, M.P., Chen, W.J.: Wave localization in multi-coupled periodic structures: application to truss beams. ASME Mech. Rev. **49**, 65–86 (1996)
8. Vakakis, A.F., Manevitch, L.I., Mikhlin, Y.V., Pilipchuk, V.N., Zevin, A.A.: Normal Modes and Localization in Nonlinear Systems. Wiley, New York (1996)
9. Gendelman, O., Vakakis, A.F.: Transitions from localization to nonlocalization in strongly nonlinear damped oscillators. Chaos Solitons Fractals **11**(10), 1535–1542 (2000)
10. Pouget, J., Remoissenet, M., Tamga, J.M.: Energy self-localization and gap local pulses in a two-dimensional nonlinear lattice. Phys. Rev. B **47**, 14866–14874 (1993)
11. Nesterov, S.V.: Examples of nonlinear Klein–Gordon equations, solvable in terms of elementary functions. Proc. Moscow Inst. Power Eng. **357**, 68–70 (1978)
12. Dimentberg, M.F., Bratus, A.S.: Bounded parametric control of random vibrations. R. Soc. Lond. Proc. Ser. A Math. Phys. Eng. Sci. **456**(2002), 2351–2363 (2000)
13. Dimentberg, M., Iourtchenko, D., Bratus, A.: Transition from planar to whirling oscillations in a certain nonlinear system. Nonlinear Dyn. **23**, 165–174 (2000)
14. Zhuravlev, V.F., Klimov, D.M.: Prikladnye metody v teorii kolebanii. Nauka, Moscow (1988) (in Russian)